



Four-and-a-half LIM domain protein 2 (FHL2) deficiency protects mice from diet-induced obesity and high FHL2 expression marks human obesity

Maria P. Clemente-Olivo^a, Jayron J. Habibe^{a,b}, Mariska Vos^a, Roelof Ottenhoff^a, Aldo Jongejan^c, Hilde Herrema^d, Noam Zelcer^a, Sander Kooijman^e, Patrick C.N. Rensen^e, Daniël H. van Raalte^f, Max Nieuwdorp^d, Etto C. Eringa^b, Carlie J. de Vries^{a,*}

^a Department of Medical Biochemistry, Amsterdam UMC, Amsterdam Cardiovascular Sciences, and Amsterdam Gastroenterology, Endocrinology and Metabolism, University of Amsterdam, Amsterdam 1105 AZ, the Netherlands

^b Department of Physiology, Amsterdam UMC, Amsterdam Cardiovascular Sciences, location VUmc, Amsterdam, the Netherlands

^c Department of Bioinformatics, Amsterdam UMC, University of Amsterdam, Amsterdam, the Netherlands

^d Department of Experimental Vascular Medicine, Amsterdam UMC, Amsterdam Cardiovascular Sciences, University of Amsterdam, Amsterdam, the Netherlands

^e Department of Medicine, Division of Endocrinology, Einthoven Laboratory for Experimental Vascular Medicine, Leiden University Medical Center, Leiden, the Netherlands

^f Department of Internal Medicine, Diabetes Center, Amsterdam UMC, Amsterdam Cardiovascular Sciences Amsterdam, the Netherlands

ARTICLE INFO

Article history:

Received 29 April 2021

Accepted 8 June 2021

Available online xxx

Keywords:

Diet-induced obese mice

Four-and-a-half LIM domain protein 2 (FHL2)

Energy metabolism

Energy expenditure

Glucose uptake

Lipid uptake

White adipose tissue (WAT)

Browning of WAT

ABSTRACT

Objective: Four-and-a-half-LIM-domain-protein 2 (FHL2) modulates multiple signal transduction pathways but has not been implicated in obesity or energy metabolism. In humans, methylation and expression of the FHL2 gene increases with age, and high FHL2 expression is associated with increased body weight in humans and mice. This led us to hypothesize that FHL2 is a determinant of diet-induced obesity.

Methods: FHL2-deficient (FHL2^{-/-}) and wild type male mice were fed a high-fat diet. Metabolic phenotyping of these mice, as well as transcriptional analysis of key metabolic tissues was performed. Correlation of the expression of FHL2 and relevant genes was assessed in datasets from white adipose tissue of individuals with and without obesity.

Results: FHL2 Deficiency protects mice from high-fat diet-induced weight gain, whereas glucose handling is normal. We observed enhanced energy expenditure, which may be explained by a combination of changes in multiple tissues; mild activation of brown adipose tissue with increased fatty acid uptake, increased cardiac glucose uptake and browning of white adipose tissue. Corroborating our findings in mice, expression of FHL2 in human white adipose tissue positively correlates with obesity and negatively with expression of browning-associated genes.

Conclusion: Our results position FHL2 as a novel regulator of obesity and energy expenditure in mice and human. Given that FHL2 expression increases during aging, we now show that low FHL2 expression associates with a healthy metabolic state.

© 2021 The Author(s). Published by Elsevier Inc. This is an open access article under the CC BY license (<http://creativecommons.org/licenses/by/4.0/>).

1. Introduction

The worldwide prevalence of obesity is reaching epidemic levels and represents a major health issue. The principal drivers in the rise of obesity are a sedentary lifestyle and an increased high-caloric food consumption, which are subject to lifestyle interventions. Obesity increases the risk for developing, among others, Type 2 Diabetes

(T2D), cardiovascular diseases and some types of cancer. However, these pathologies do not always develop in subjects with obesity, because other genetic and environmental factors contribute substantially to their etiology. Many genes have been correlated to body-mass index, a proxy for obesity, but only a small proportion of these genes has been directly positioned within specific biological pathways [1].

In addition to genetic factors, current evidence supports the notion that epigenetics, and specifically DNA methylation, play a role in obesity and associated comorbidities [2]. Hypermethylation of certain DNA regions is characteristic of the aging process, and it is well-recognized that obesity is highly prevalent among the elderly. Moreover, it has

* Corresponding author at: Department of Medical Biochemistry, Location AMC, room K1-113, Meibergdreef 15, 1105AZ Amsterdam, the Netherlands.
E-mail address: c.j.devries@amsterdamumc.nl (C.J. de Vries).

been hypothesized that obesity can promote epigenetic aging in metabolic tissues, something that so far has been proven in the liver [3,4]. In humans, consistent age-related DNA hypermethylation of the LIM-only-protein-Four-and-a-Half LIM domain protein 2 (FHL2) gene is observed in blood cells, white adipose tissue (WAT), liver and pancreatic islets [5–7]. Notably, increased methylation in the FHL2 locus itself results in increased FHL2 expression [6].

FHL2 is a protein that integrates signaling pathways to regulate transcriptional responses through its association with an array of target proteins in a signal- and cell-dependent manner [8]. FHL2 is expressed in several organs and cell types throughout the body. Its expression is highest in the heart, which prompted investigation of its role in cardiac function [9]. Whole-body FHL2-deficient mice (FHL2^{-/-}) are viable and have normal cardiac development and function. However, these mice show an exaggerated response upon induction of cardiac hypertrophy as compared to wild type mice. Whether FHL2 plays a role in energy metabolism is largely unknown. However, anecdotal reports implicate a role for FHL2 in fatty acid and cholesterol metabolism [10,11]. This has prompted us to address the role of FHL2 in whole body energy metabolism and obesity.

We report here that FHL2-deficient mice are protected from high-fat diet (HFD)-induced obesity and posit that this can be attributed to increased lipid uptake by brown adipose tissue (BAT), increased uptake of glucose by the heart and a marked browning of WAT. Importantly, to substantiate the results in mice, our analysis of human cohorts revealed that FHL2 expression in WAT correlates positively with obesity, and negatively with expression of browning genes. Together, our data position the signal transduction intermediary protein FHL2 as a novel modifier of obesity.

2. Materials and methods

2.1. Human data analysis

The publicly accessible human datasets used in this study were: a) GSE59034, from subcutaneous white adipose tissue from female individuals before going through bariatric surgery ($n = 16$) and lean controls that never had obesity ($n = 16$) [12], and b) GSE70353, from subcutaneous white adipose tissue of 770 male individuals (age: 45–73 years old) with varying BMI who were part of the METSIM study [13,14]. These datasets were uploaded to R2: Genomics Analysis and Visualization Platform (<http://r2.amc.nl>) for analysis. Analysis for genes that significantly associate with FHL2 expression was performed using this software.

2.2. F2 intercross mice study (BHF2) dataset analysis

Dataset from F2 intercross between C57BL/6 and C3H/HeJ mice on ApoE^{-/-} background (BHF2 population) generated at The University of California Los Angeles (UCLA) was retrieved from the publicly available GeneNetwork database (<http://www.genenetwork.org>). Pearson correlations were obtained from male mice adipose tissue mRNA and described phenotypes.

2.3. Mouse strains

All animal experiments were approved by an ethic committee of the Amsterdam University Medical Center, The Netherlands (permit number DBC287) and were performed in accordance with European directive 2010/63/EU guidelines. Working protocols for every experiment reported here were approved by the ethic committee of the Amsterdam University Medical Center. FHL2-deficient mice were generated by R. Bassel-Duby (University of Texas Southwestern Medical Center, Dallas, TX) and were bred onto a C57BL/6 background for more than 11 generations. In all experiments, male littermates of 8- to 20-week-old were used and n refers to the number of single animals. We did not include female mice in our study because

of the knowledge that especially female mice have a bone defect upon FHL2 deficiency, which may affect body weight [15]. Sample size for each experiment was determined by power calculation using the nQuery software (<https://www.statsols.com/>). Littermates from wild-type and FHL2-deficient genotype were randomly separated in ventilated cages with free access to water and food (60% fat diet Open Source diets #D12492). High-fat diet feeding was started at the age of 8–10 weeks. Mice were terminated by intraperitoneal injection of a lethal dose of ketamine (166 mg/kg) plus xylazine (24 mg/kg). Both number and suffering of animals was minimized as much as possible, such as group housing except for the metabolic cage experiments and cage enrichment. Health was monitored weekly by researchers and animal caretakers and humane endpoints were taken into account under standard procedure from the animal research facility. After termination, mouse tissues were rinsed with ice-cold PBS through trans-cardiac perfusion, harvested and stored at -80°C for further analysis.

2.4. Glucose and insulin tolerance

For the intraperitoneal glucose tolerance test (ipGTT), mice were fasted 4 h prior receiving an injection of glucose (2 g/kg body weight). For insulin tolerance tests (ITT), mice were fasted for 4 h prior injection of an intraperitoneal insulin dose (1 IU/kg body weight, Sigma Aldrich). In all experiments blood was collected from the tail vein at baseline and every 15 min for a period of 120 min. Blood glucose was measured using an automatic Stat Strip glucometer (Nova Biomedical). At indicated times, blood samples were collected in EDTA-coated capillary tubes, centrifuged and plasma samples were stored at -80°C for further measurements.

2.5. Biochemical analyses

Mouse blood was collected from the tail vein using EDTA-coated capillary tubes after 4 h of fasting. Blood was centrifuged at room temperature and plasma was isolated and stored at -80°C until analysis. Plasma triglyceride (TG), total cholesterol (TC), adiponectin and leptin levels were measured using: Triglyceride GPO Method Assay Kit (Biolabo), Cholesterol CHOD-PAP Method Assay kit (Biolabo), mouse adiponectin ELISA kit (Crystal Chem) and mouse leptin ELISA kit (Crystal Chem), respectively, following the manufacturer's protocols.

2.6. Absorption of dietary fat

Dietary fat absorption was measured in 4 h fasted chow- or HFD-fed mice at noon. Plasma triglycerides were measured before and after an oral bolus of olive oil (400 μl) administered by intragastric gavage; blood samples were taken at indicated time points.

2.7. Fecal energy and lipid extraction

To measure fecal energy and lipid content, 24 h feces was collected from individually housed mice to quantitatively determine food intake and feces production. Feces were weighed, freeze-dried, and grinded prior to analysis. First, in order to measure the energy excreted, feces from 3 mice was pooled in a total of 3 measurable samples. A bomb calorimeter (IKA C1) was used for combustion and a food sample was taken along as reference (Lovelady and Stork, 1970).

Fecal lipids were extracted from freeze-dried feces in a mixture of methanol and 10 M NaOH and incubated at 90°C . Afterwards, a solution of 6 M HCl and hexane was added for lipid solubilization. After centrifugation, a second step of hexane was needed before the samples were dried under a nitrogen stream at 40°C and dissolved in 2% Triton X-100. Triglycerides and total cholesterol were measured as described in the previous section. Non-esterified fatty acids (NEFA) were measured using HR Series NEFA-HR(2) (Wako Diagnostics).

2.8. Indirect calorimetry

Wild type and FHL2^{-/-} mice were randomly and individually housed in PhenoMaster Indirect Calorimetry System (TSE Systems, Bad Homburg, Germany) for 5 days where they had access to food and water ad libitum. Mice adapted to the PhenoMaster system for 48 h before the start of data analysis. The measurements in the metabolic cages are performed automatically, so that blinding is not necessary. Allocation and measurements were performed at the same time for wild type and FHL2^{-/-} mice. Here, we analyzed bodyweight, locomotor activity, respiratory exchange ratio (RER), O₂ consumption and CO₂ production, energy expenditure (EE). Rates of oxygen consumption (VO₂, ml/h) and carbon dioxide production (VCO₂, ml/h) were calculated by TSE software and used to calculate the RER ($RER = VCO_2/VO_2$) and EE (kcal/h). Locomotor activity was measured by infrared beams at the long side (X-frame) and at the short side (Y-frame) of the cage (expressed as total beam breaks (both X and Y) per hour). Energy Expenditure (EE) ANCOVA analysis was performed using the Energy Expenditure Analysis page (<http://www.mmmpc.org/shared/regression.aspx>) of the NIDDK Mouse Metabolic Phenotyping Centers (MMPC).

2.9. Histology

Organs were fixed in 4% paraformaldehyde (Roth), embedded in paraffin, sectioned and mounted onto StarFrost glass slides (Thermo Scientific). Sections (5 μm thickness) were deparaffinized and rehydrated. Tissue morphology was assessed by hematoxylin and eosin staining (H&E) (Sigma). Sections were visualized with a Leica DM6 microscope and quantified using Leica LAS-X Software. Sectioning and staining was performed by a researcher and lipid content quantification of histological sections was performed blindly by another researcher.

2.10. In vivo triglyceride and glucose clearance

TG-rich lipoprotein (TRL)-like particles (80 nm), radiolabeled with glycerol tri[³H]oleate (3.7 MBq) were prepared as described before (Li et al., 2020), and stored at 4 °C under argon until use at the second day after preparation. TRL-like particles were mixed 2-[¹⁻¹⁴C]deoxy-D-glucose ([¹⁴C]DG) in a 4:1 ratio (³H:¹⁴C). Mice at 12 weeks old (4 weeks of HFD) were injected via the tail vein with the combination of TRL-like particles (1 mg TG) and deoxyglucose (200 μL/mouse). After 15 min, mice were killed by CO₂ inhalation, transcardially perfused with ice-cold PBS, tissue was collected and a piece was dissolved in 500 μL of Solvable (Perkin Elmer) overnight at 56 °C. The tissue uptake of ³H and ¹⁴C was determined using scintillation counting (Ultima Gold XR, Perkin Elmer).

2.11. RNA extraction and reverse transcription (RT)-qPCR

Total RNA was isolated using Trizol reagent (Invitrogen) according to the manufacturer's protocol. cDNA was synthesized using iScript cDNA synthesis kit (BioRad). Quantitative PCR was carried out using SensiFAST SYBR No-ROX Kit (Bioline) on a LightCycler 480 II PCR platform (Roche). Cycle quantification and primer set amplification efficiency were calculated using the LinRegPCR software package (Ruijter et al., 2009). Target gene expression was normalized by dividing the geometric mean of the gene expression of Rplp0 and β-actin. Primer sequences are listed in Table S1.

2.12. Western blotting

Frozen tissue samples were powdered in liquid nitrogen. Proteins were isolated using RIPA buffer (150 mM NaCl, 50 mM Tris pH 7.4, 1% Nonidet-P40, 0.5% sodiumdeoxycholate, 0.1% SDS and Roche cComplete™ protease inhibitor cocktail) and quantified using the DC

protein assay (BioRad). Equal amounts of protein lysate were loaded on to 12% SDS-PAGE gels along with the protein ladder standard (Precision Plus Protein™ All Blue Prestained Protein Standards from Bio Rad) and transferred to nitrocellulose membranes. Membranes were blocked with 5–10% non-fat milk for 1 h and subsequently incubated with primary antibody (Rabbit anti-UCP1; Abcam #ab10983 and Mouse anti-alpha-tubulin; Cedarlane #CLT9002 as loading control) at 4 °C overnight. Membranes were washed and incubated with appropriate HRP-conjugated secondary antibodies for 1 h at room temperature and protein bands were visualized using Supersignal West Pico PLUS Chemiluminescent Substrate (Thermo Scientific) and ImageQuant LAS 4000 imager (GE Healthcare). Quantification of band intensity was performed with reference to loading control (alpha-tubulin) using ImageJ Gel Analysis program.

2.13. Differentiation of pre-adipocytes from the stromal vascular fraction of white adipose tissue

Pre-adipocytes from the stromal vascular fraction (SVF) of white adipose tissue (WAT) were isolated from WT and FHL2^{-/-} mice white. Fat pads were minced in 1.5 mg/ml collagenase solution (Sigma-Aldrich; #C6885) and homogenates were digested for 60 min at 37 °C on a shaking platform. After digestion, homogenates were filtered through a 100 μm strainer and centrifuged at 1600 rpm for 10 min. Cell pellets were resuspended in red blood cell lysis buffer (Roche; #11814389001) and neutralized with DMEM supplemented with 10% FBS and 1% penicillin-streptomycin. Cells were again centrifuged at 1200 rpm for 5 min and seeded in cell culture plates for differentiation. When cells reached full confluency they were cultured for two more days before the addition of culture medium supplemented with 3-isobutyl-1-methylxanthine (500 μM), dexamethasone (1 μM), insulin (170 nM) and rosiglitazone (1 μM) to induce differentiation. After this, every two days medium supplemented only with insulin was added and left until day 8 of differentiation where RNA was isolated and Oil Red O staining was performed.

2.14. RNA sequencing (RNA-seq)

Heart and gonadal (g)WAT of 4 HFD wild-type and 4 HFD FHL2^{-/-} mice ($n = 3$ in case of gWAT) were used for mRNA isolation using Trizol reagent (Invitrogen) according to the manufacturer's protocol. RNA concentration was measured using the Nanodrop ND-1000 spectrophotometer (Nanodrop Technologies) and RNA quality was determined using the Eukaryote Total RNA Nano assay from Agilent 2100 Bioanalyzer (Agilent Technologies). Strand-specific libraries were generated using the Kapa mRNA Hyperprep kit (Roche). Libraries were sequenced on an Illumina HiSeq4000 in single-end 50 bp reads. Reads were subjected to quality control (FastQC, dupRadar, Picard Tools), trimmed using Trimmomatic v0.32 and aligned to the genomes using HISAT2 (v2.1.0). Counts were obtained using HTSeq (v0.11.0) using the corresponding GTFs [20–22]. Statistical analyses were performed using the edgeR and limma/voom R packages [23,24]. Count data were transformed to log₂-counts per million (logCPM), normalized by applying the trimmed mean of M-values method and precision weighted using voom. Differential expression was assessed using an empirical Bayes moderated *t*-test within limma's linear model framework including the precision weights estimated by voom. Resulting *P* values were corrected for multiple testing using the Benjamini-Hochberg false discovery rate. Genes were re-annotated using biomaRt using the Ensembl genome databases. Geneset enrichment is performed with MSigDB genesets using CAMERA approach as implemented in limma. The resulting DEGs, expression plots, geneset enrichment results are shown in an in-house made Shiny-app. Ingenuity Pathway Analysis (IPA) was used to identify the significant canonical pathways arising from the gene expression changes observed. Only genes with a differential expression of adjusted *p*-value <0.05 were included in the analysis.

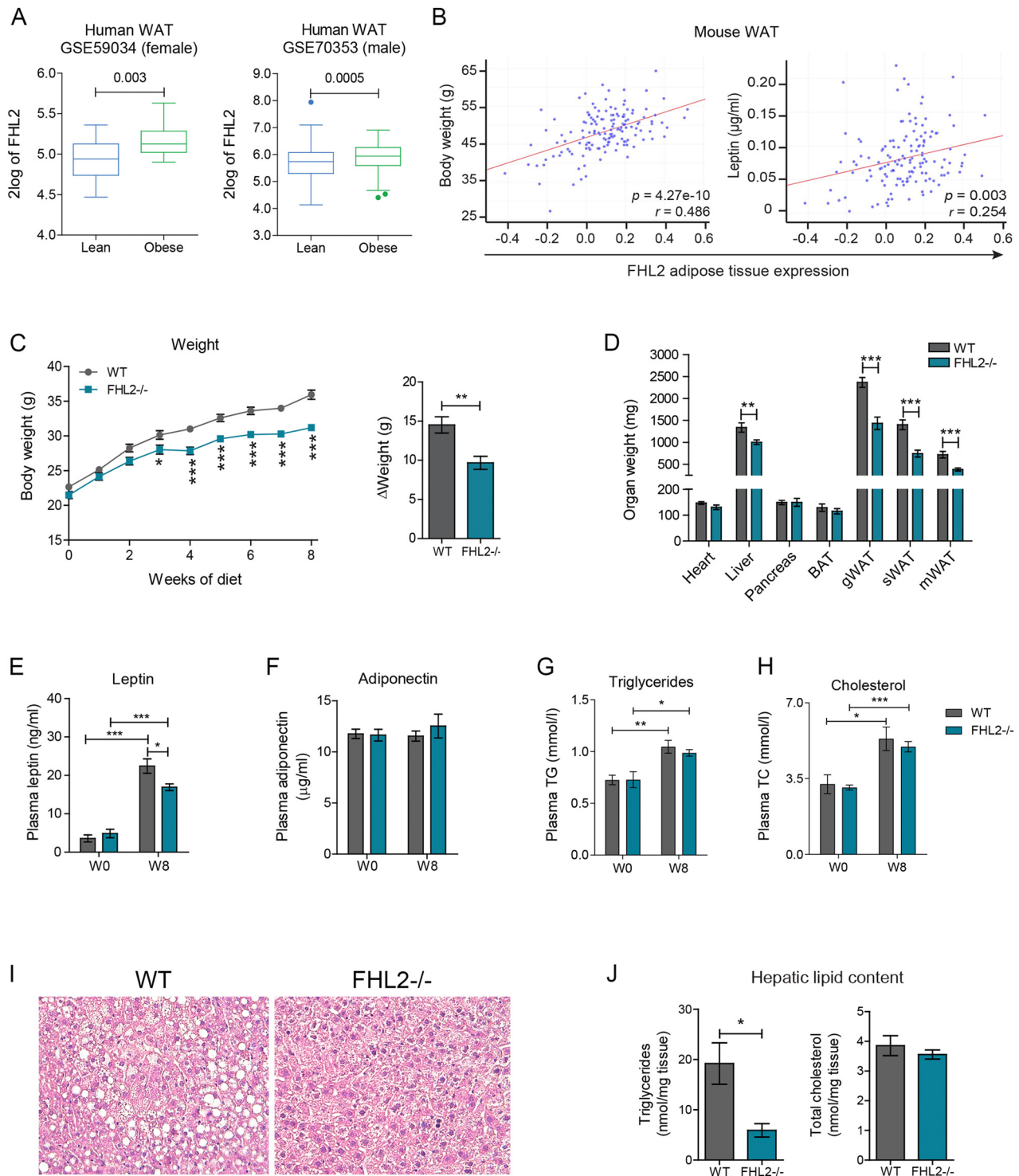


Fig. 1. FHL2 expression increases with body weight and FHL2-deficient mice are protected from diet-induced obesity.

(A) FHL2 expression in human adipose tissue is higher in individuals with obesity (green) than in lean (blue) individuals from two different cohorts. GSE59304: female cohort, lean individuals ($n = 16$) and individuals with obesity ($n = 16$). GSE70353: male cohort, lean individuals ($n = 259$) and individuals with obesity ($n = 110$). Outliers are depicted by individual circles.

(B) Positive correlation between FHL2 expression in mouse white adipose tissue (WAT) and bodyweight or leptin levels from an F2 intercross study (BHF2 population).

(C) Body weight and weight gain (Δ Weight) of WT and FHL2^{-/-} mice after 8 weeks of HFD ($n = 7$).

(D) Weight of isolated organs of mice after 8 weeks of HFD ($n = 7$).

(E) Plasma leptin levels at the onset (W0) and after 8 weeks (W8) of HFD.

(F) Plasma adiponectin levels at the onset (W0) and after 8 weeks (W8) of HFD.

(G) Plasma triglycerides at the onset (W0) and after 8 weeks (W8) of HFD.

(H) Plasma total cholesterol at the onset (W0) and after 8 weeks (W8) of HFD.

(I) H&E staining of liver tissue ($n = 3$).

(J) Hepatic lipid content of triglycerides and cholesterol ($n = 4$).

Data are indicated as mean \pm SEM. p -values were calculated using two-tailed Student's t -test or two-way ANOVA with Tukey post-hoc test. * $p < 0.05$; ** $p < 0.01$; *** $p < 0.001$. See also supplemental data in Fig. S1 and S2. (For interpretation of the references to colour in this figure legend, the reader is referred to the web version of this article.)

The raw and processed RNA-seq data have been deposited in the Gene Expression Omnibus (GEO) database under accession number GSE156027.

2.15. Statistical analysis

Statistical analyses were performed using GraphPad Prism software. Data are reported as mean \pm SEM. Two-tailed unpaired Student's *t*-test was used when comparing two groups and Two-way analysis of variance (ANOVA) was used to analyze time course experiments, with a *p*-value <0.05 being considered significant and levels of significance being indicated as follows: **p* <0.05 ; ***p* <0.01 ; ****p* <0.001 .

3. Results

3.1. FHL2 expression in adipose tissue correlates with body weight in mice and men and FHL2-deficient mice are resistant to high-fat diet-induced weight gain

Analysis of a publicly available gene expression dataset of white adipose tissue (WAT) from individuals with and without obesity revealed higher FHL2 expression in individuals with obesity. Higher FHL2 expression could be confirmed in a second dataset of WAT from a different cohort (Fig. 1A). The first cohort (GSE59034) consisted of 16 women with obesity before undergoing bariatric surgery and 16 lean women as control, whereas the second cohort (GSE70353) comprised 770 male individuals with variable BMI [12,14]. In the latter database, we separated the data in groups according to their BMI in lean individuals (BMI <25 kg/m²; *n* = 259) and individuals with obesity (BMI >30 kg/m²; *n* = 110) [16]. Mouse hybrid panels are a powerful tool to dissect genotype-phenotype associations. Therefore, we also explored the contribution of FHL2 expression to metabolic parameters in a well-characterized F2 intercross between C57BL/6 and C3H/HeJ mice on an ApoE^{-/-} background [17], using the public database GeneNetwork [18]. Analysis of FHL2 expression in mouse WAT revealed a strong positive correlation between FHL2 expression and both body weight and leptin levels (Fig. 1B). These observations support our hypothesis that FHL2 may play a role in development of obesity.

To explore this further, we fed WT and FHL2-deficient (FHL2^{-/-}) littermate mice a high-fat diet (HFD) for eight weeks. FHL2-deficient mice fed a HFD were markedly protected from weight gain (Fig. 1C). This was dependent on the HFD, since we observed no difference in weight gain between WT and FHL2^{-/-} mice fed a chow diet (Fig. S1A). For this reason we subsequently focused on HFD mice in this study. Food intake could not explain the difference in weight gain as it was similar between the HFD-fed groups (Fig. S1B). Notably, the reduced overall body weight gain coincided with a reduction in the weight of WAT, in all three different depots examined: gonadal (gWAT), subcutaneous (sWAT) and mesenteric (mWAT) fat (Fig. 1D), in addition to a decreased liver weight. This was further reflected by lower circulating leptin plasma levels (Fig. 1E), although adiponectin remained unaltered (Fig. 1E-F). Fasting levels of plasma triglycerides and cholesterol were comparable between the groups after 8 weeks of HFD (Fig. 1G-H). The observation that FHL2-deficient mice have a lower liver weight, prompted us to evaluate the morphology of this tissue (Fig. 1I). This analysis revealed reduced neutral lipid accumulation in FHL2^{-/-} hepatocytes, which could be attributed specifically to decreased triglyceride accumulation (Fig. 1J).

Having ruled out food intake as the primary cause for reduced weight gain in FHL2^{-/-} mice we considered the possibility that these mice have enhanced calorie loss via the fecal excretion route. However, here too we observed no difference in fecal output and fecal caloric density over a period of 24 h between the groups (Fig. S1C, D). With this information, caloric absorption and caloric loss could be calculated and were also not different (Fig. S2E-F), as well as fecal lipid content (Fig. S1G). At face value, this indicates that the observed reduced

weight gain was not secondary to reduced absorption of calories or their increased fecal excretion. Next, we examined whether the reason was a different handling of TG upon intestinal absorption. To this end, fasted mice received an oral bolus of olive oil and TG in plasma was measured for up to for 4 h. Under this experimental setting we observed no difference in plasma TG excursions between the groups (Fig. S1H).

3.2. HFD-challenged FHL2-deficient mice show unaltered glucose handling

Obesity is an important driver of hyperglycemia and insulin resistance [19]. Both at baseline, and following 8 weeks of HFD, fasted plasma glucose levels in FHL2^{-/-} mice were lower than in WT mice (Fig. 2A). Glucose clearance was addressed by an intraperitoneal glucose tolerance test (ipGTT) after HFD, and was only statistically significant at the 120-minute time point after glucose administration (Fig. 2B). The area under the curve of the ipGTT was, however, similar for WT and FHL2^{-/-} mice (Fig. 2B). Insulin levels during the ipGTT were only significantly lower in FHL2^{-/-} mice at the onset of this experiment. (Fig. 2C). Importantly, an insulin tolerance test (ITT) did not reveal a significant difference in insulin sensitivity between the groups (Fig. 2D). In conclusion, glucose clearance and insulin resistance is comparable between WT and FHL2^{-/-} mice after a HFD.

3.3. Increased energy expenditure in FHL2-deficient mice

Since caloric intake was unaffected, enhanced energy expenditure may explain resistance to diet-induced obesity in FHL2^{-/-} mice. To evaluate this possibility, we placed HFD-fed WT and FHL2^{-/-} mice in metabolic cages and used indirect calorimetry analysis to determine their energy expenditure. Analysis of locomotor activity, which includes both horizontal and vertical movements, revealed that FHL2^{-/-} mice were more stationary than WT mice (Fig. 3A). This suggests that physical activity or changes in skeletal muscle metabolism are an unlikely explanation for the reduced weight gain of HFD-fed FHL2^{-/-} mice.

Overall substrate utilization, as inferred from the respiratory exchange ratio (RER), did not differ between groups, implying that fat was the main energy source used by the mice (Fig. 3B). Interestingly, energy expenditure, or heat production, was higher in FHL2^{-/-} mice as evident also from their increased O₂ consumption and subsequent CO₂ production (Fig. 3C-D). To discard bodyweight as a confounding factor of energy expenditure measurements, we also plotted the energy expenditure data from individual mice against their specific bodyweight. Making use of the analysis of covariance (ANCOVA test) we confirmed that bodyweight was not a confounder, and that the significant difference in energy expenditure was independent of this variant (Fig. S2A-B). Hence, increased energy expenditure indeed likely contributes to the leaner phenotype in FHL2^{-/-} mice.

Accordingly, when we measured glucose and lipid uptake by different tissues by injecting [¹⁴C]-deoxyglucose and TG-rich lipoprotein-like particles containing glycerol tri-³H-oleate in fasted mice, we found a significant preference for lipid uptake by BAT of FHL2^{-/-} mice (Fig. 3E). The preference for lipids in absence of FHL2, albeit not significant, may hint at higher fat oxidation activity in this tissue (Fig. S3A-B). Since BAT is one of the main organs in control of energy expenditure, at least in the mouse, this could partially explain the increase in energy expenditure as we observed for FHL2^{-/-} mice.

3.4. FHL2 deficiency increases cardiac glucose utilization

FHL2 expression is high in cardiomyocytes, but can also be found in smooth muscle cells and endothelial cells, where it exerts a variety of functions [20,21]. Since the heart contributes notably to the whole-body energy expenditure [22], we further analyzed the heart of HFD-fed mice.

Under normal conditions the heart relies primarily on fatty acid oxidation for its energy supply but this changes when cardiac pathologies

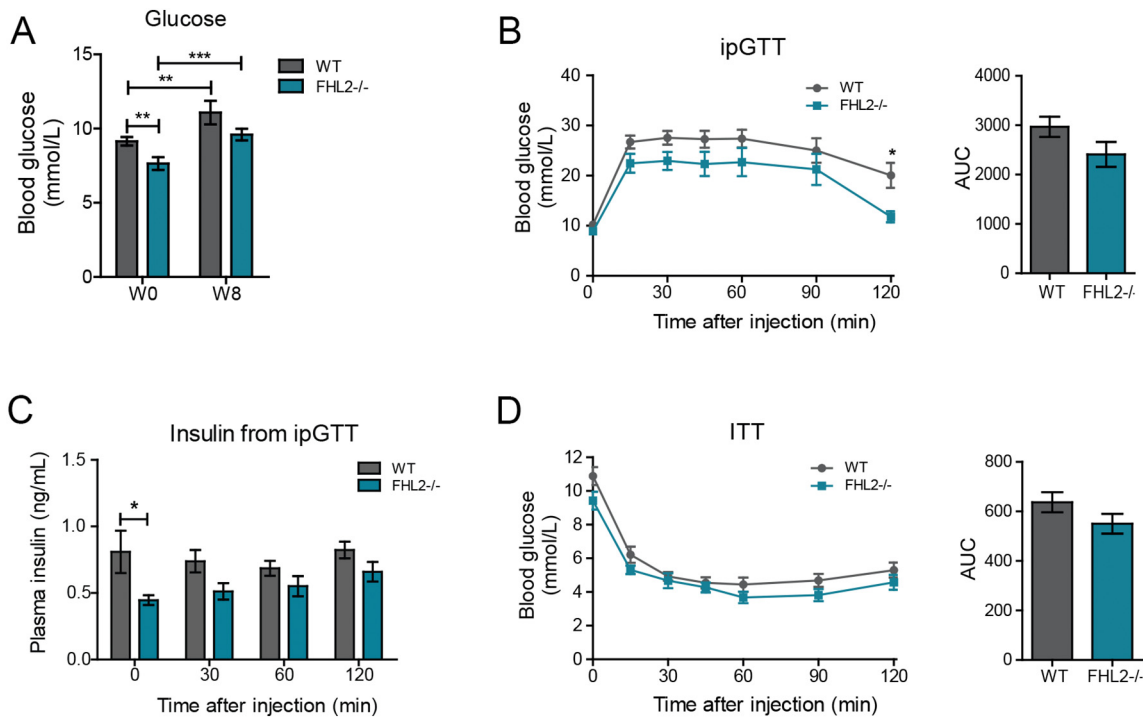


Fig. 2. HFD-challenged FHL2-deficient mice show unaltered glucose handling.

(A) Plasma glucose levels at the onset (W0) and after 8 weeks of HFD (W8) (n = 7).

(B) Intraperitoneal glucose tolerance test (ipGTT) and area under curve (AUC) (n = 7).

(C) Plasma insulin levels during ipGTT.

(D) Intraperitoneal insulin tolerance test (ITT) and area under curve (AUC) (n = 7).

Data are indicated as mean ± SEM. p-values were calculated using two-tailed Student's *t*-test or two-way ANOVA with Tukey post-hoc test. *p < 0.05; **p < 0.01; ***p < 0.001.

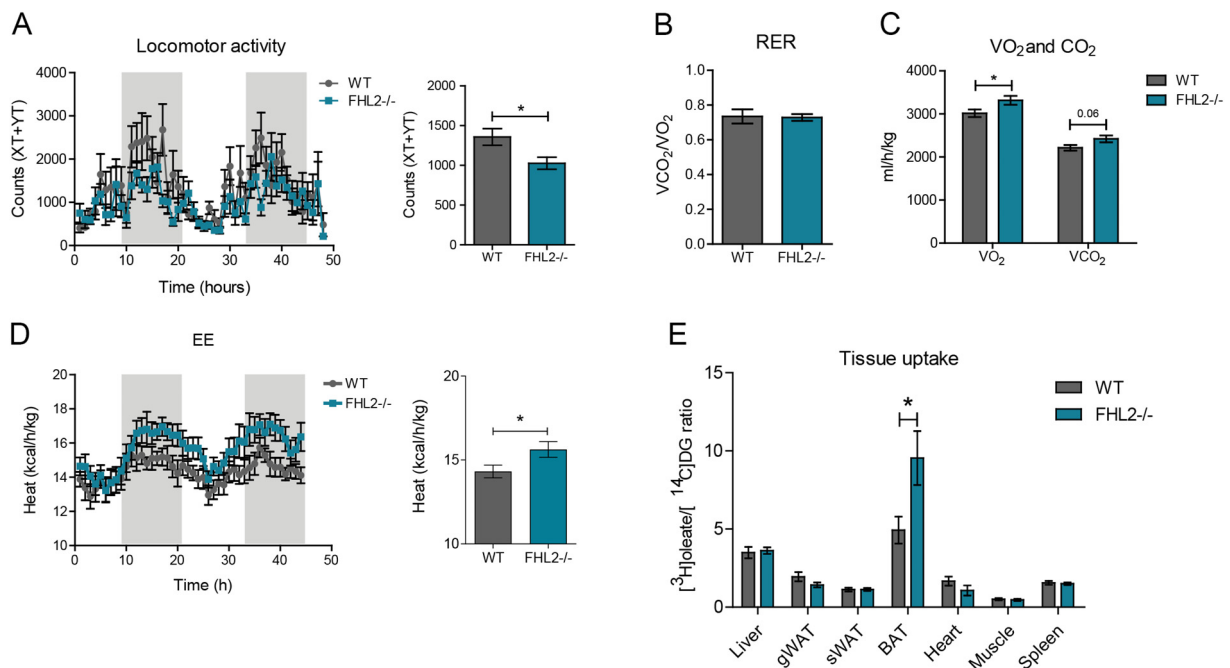


Fig. 3. Indirect calorimetry reveals enhanced energy expenditure in FHL2^{-/-} mice.

(A) Locomotor activity (48 h) and average activity.

(B) Average respiratory exchange ratio (RER).

(C) Average O₂ consumption and CO₂ production.

(D) Heat or energy expenditure (EE) in time for 48 h and average EE (WT n = 11, FHL2^{-/-} n = 12).

(E) Ratio of the uptake of glycerol tri[³H]oleate and [¹⁴C]deoxyglucose per mg of metabolic tissues of fasted mice after 4 weeks of high fat diet (HFD; WT n = 7, FHL2^{-/-} n = 9).

Data are indicated as mean ± SEM. p-values were calculated using two-tailed Student's *t*-test or two-way ANOVA with Tukey post-hoc test. *p < 0.05; **p < 0.01; ***p < 0.001. See also Fig. S3.

arise, shifting energy utilization towards glucose as the preferential substrate [23,24]. In our model we found that glucose uptake was higher in FHL2^{-/-} hearts (Fig. 4A) after 4 weeks of HFD. This was particularly

interesting given the already described involvement of FHL2 in cardiac hypertrophic response after a challenge [9]. Transcriptome analysis (RNA-seq) on ventricular heart tissue from WT and FHL2^{-/-} mice

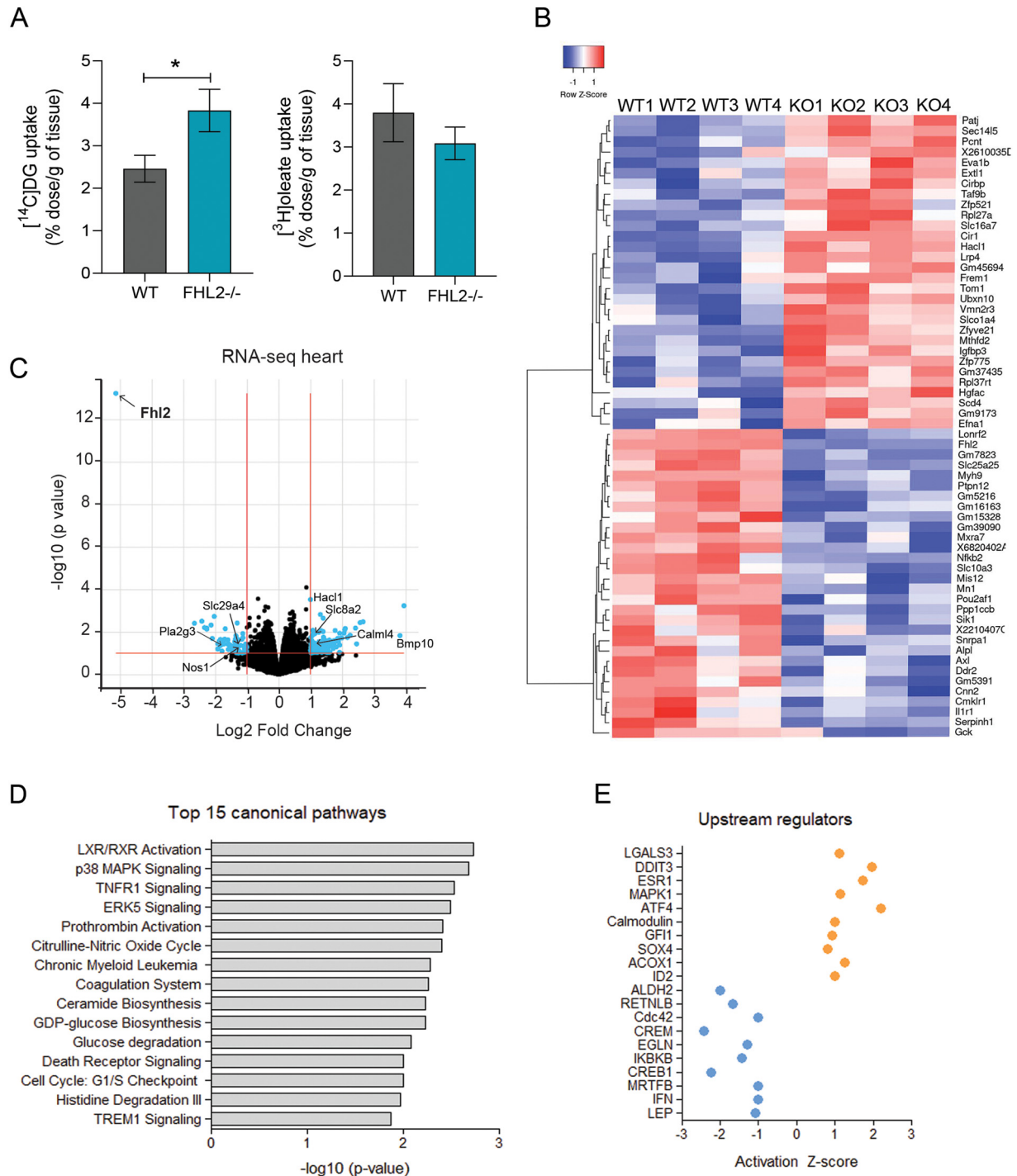


Fig. 4. Metabolite usage and gene expression in the heart of WT and FHL2^{-/-} mice after HFD.

(A) Uptake of [^{14}C]deoxyglucose (DG) and glycerol tri[^3H]oleate in the heart of fasted mice that received 4 weeks of high fat diet ($n = 8$).

(B) Heatmap of the top 30 up- and down-regulated genes in FHL2^{-/-} versus WT heart ($n = 4$).

(C) Volcano plot of genome-wide RNA-seq data of FHL2^{-/-} versus WT heart; in blue, genes with >2 -fold change of expression and p -value < 0.05 . The arrows indicates individual data for a selected set of gene expression.

(D) Top 15 most significant canonical pathways from Ingenuity Pathway Analysis (IPA) of FHL2^{-/-} versus WT hearts.

(E) IPA upstream regulator analysis results showing significantly activated regulators in orange and significantly inhibited regulators in blue. Order by activation score (Z-score) of specific target genes differentially expressed in this dataset.

Data are indicated as mean \pm SEM. p -values were calculated using two-tailed Student's t -test. * $p < 0.05$; ** $p < 0.01$; *** $p < 0.001$. (For interpretation of the references to colour in this figure legend, the reader is referred to the web version of this article.)

provided further evidence of transcriptional changes in the absence of FHL2 (Fig. 4B, C; Table S2). In Fig. 4C the remarkably high FHL2 expression level in the heart can be appreciated by comparing it to other differentially expressed genes. The use of Ingenuity Pathway Analysis (IPA) revealed the liver X nuclear receptor (LXR)/retinoid X receptor (RXR) pathway as the most significantly altered pathway in FHL2^{-/-} in comparison to WT heart (Fig. 4D). The finding is consistent with our earlier report that identifies FHL2 as a transcriptional coactivator of both LXR isoforms (LXR α and LXR β) [11]. Interestingly, we found MAPK and ERK signaling, which have a key role in cardiac hypertrophy, within the top regulated pathways as well. In line with our observation of increased glucose uptake by the heart, glucose metabolism pathways were also among the most altered pathways in absence of FHL2. Moreover, when looking at the upstream regulators based on gene expression differences (Fig. 4E), we found among the most significant activated regulators some that are involved in the cellular response to stress, such as DDIT3 and ATF4 [25,26], cardiac hypertrophy and heart failure like MAPK1 and LGALS3 [27,28].

3.5. Brown adipose tissue is comparable in FHL2-deficient and wild type mice

Given that non-shivering heat production takes place in thermogenic tissues including brown adipose tissue (BAT) and in WAT upon browning, we first analyzed BAT in detail looking for a potential explanation for the increase in energy expenditure. Histological analyses revealed that brown adipocyte morphology and total lipid area did not differ between groups (Fig. 5A–B). Moreover, the expression of uncoupling protein 1 (Ucp1) and a set of other thermogenic genes was comparable between WT and FHL2^{-/-} mice (Fig. 5C). We found a slight but nonsignificant increase in expression of genes related to lipid handling, such as lipoprotein lipase (Lpl) and adiponectin (Adipoq) in the absence of FHL2. At protein level, we observed a trend towards increased UCP1 protein expression (Fig. 5D). These results, together with the substrate preference as shown in Fig. 3E, suggest that a change in BAT activity in FHL2^{-/-} mice may make a small, though potentially relevant contribution to improved metabolic function in the HFD challenge.

3.6. FHL2-deficient mice show increased browning of white adipose tissue

In line with reduced weight gain, WAT mass was significantly reduced in FHL2^{-/-} compared to WT mice (Fig. 1C). To assess whether FHL2 deficiency leads to structural differences in this tissue, histological staining and subsequent quantification was performed for three WAT depots; gWAT, sWAT and mWAT (Figs. 6A, S4A–C). Adipocyte morphology, size and number differ between WAT compartments, matching previous observations [29]. Only in gWAT, a significant difference was observed in adipocyte size between WT and FHL2^{-/-} mice (Fig. 6A). To find functional differences between WT and FHL2^{-/-} gWAT, the expression of genes involved in adipogenesis and adipocyte maintenance was determined. The expression of the adipogenic master regulator peroxisome proliferator-activated receptor gamma (Pparg) is decreased, as well as that of leptin (Lep) (Fig. 6B). In addition, peroxisome proliferator-activated receptor gamma coactivator 1-alpha (Pgc1a), whose function is linked to mitochondrial biogenesis and adaptive response to external stimuli, is profoundly increased in gWAT of FHL2^{-/-} mice.

To map the global transcriptional changes induced by loss of FHL2 we performed RNA-seq analysis of WAT (Figs. 6E, S4E and Table S3). Gene set analysis identified a number of pathways that were significantly different between genotypes (Fig. 6D). Within the top pathways we found iron homeostasis signaling and glutathione-mediated detoxification, which interestingly, have been described to play a role in adipocyte thermogenesis [30,31]. Therefore, we hypothesized that thermogenesis-related genes might be increased in gWAT and to test

this, the newly developed BATLAS software was used to analyze our RNA-seq data [32]. This algorithm calculates the brown adipocyte gene signature in a given tissue using transcriptional profiles as input. BATLAS analysis revealed a significant higher content of browning genes in FHL2^{-/-} gWAT (Fig. 6F). Interestingly, our RNA-seq results confirmed an upregulation of the β 3-adrenergic receptor (Adrb3) (Fig. 6G), whose activation is known to induce browning of white adipose tissue [33], as well as its lipolytic target genes adipose triglyceride lipase (Atgl) and hormone-sensitive lipase (Hsl). Expression of other factors that have already been described to be essential or involved in browning of white adipocytes, such as early B cell factor 2 (Ebf2), spectrin repeat containing nuclear envelope protein 2 (Syne2), bone morphogenetic protein 4 and 7 (Bmp4, Bmp7) and Epithelial V-Like Antigen 1 (Eva1) were also higher in GWAT of FHL2^{-/-} mice (Fig. 6G) [32,34–38].

Given the differences in adipocyte gene expression, we decided to test if the differentiation capacity of pre-adipocytes from the stromal vascular fraction (SVF) was different between WT and FHL2^{-/-} mice. After pre-adipocyte isolation and differentiation *in vitro* we found no differences in lipid accumulation, as well as in adipogenesis related gene expression after 8 days. Interestingly, we observed a consistent but non-significant upregulation of Pgc1a expression in the absence of FHL2, which may indicate that even cultured adipocytes tend to show browning upon FHL2 deficiency (Figs. 6C, S4D). Taken together, we propose that increased browning of WAT contributes substantially to the observed increase in energy expenditure in FHL2^{-/-} mice (Fig. 4D).

3.7. Correlation between expression of FHL2 and markers of browning in human WAT

As FHL2 expression is increased in WAT of individuals with obesity (Fig. 1A) we expanded and extrapolated our findings in mice to human. To do so, we evaluated the correlation between expression of FHL2 and several genes which are known to participate in the browning of WAT in adipose tissue from the cohorts described in GSE59034 and GSE70353 [12,14] (Fig. 1A). PGC1 α , as well as other factors involved in the process of browning of white adipocytes, such as cardioprotein synthase 1 (CRLS1), sirtuin 1 (SIRT1), PPAR γ and BMP7 all showed a significant negative correlation with FHL2 expression in human WAT (Fig. 7A; Table S4) [37–41]. Reciprocally, genes whose expression has been described to negatively affect WAT browning correlated positively with FHL2 expression. Among these genes are transforming growth factor beta 1 (TGFB1), Ab-hydrolase domain containing 6 (ABDH6) and zinc family member 1 (ZIC1) (Fig. 7B) [42–44]. Finally, we looked for the correlation of FHL2 expression with expression of these genes in the second cohort (GSE70353), where we also validated the results for most of the genes. Moreover, in this dataset also UCP1 showed a significant negative correlation with FHL2 expression, as well as another relevant browning marker, the surface marker purinergic receptor P2X5 (P2RX5) (Table S4). Taken together, and in line with our study in mice, we observed in human WAT a reciprocal correlation between expression of FHL2 and a broad panel of browning genes in lean and individuals with obesity (Fig. S5).

4. Discussion

In this study, we demonstrate to our knowledge for the first time that FHL2 expression is higher in WAT of individuals with obesity compared to lean humans. In addition, we prove that FHL2-deficient mice have an improved metabolic phenotype in response to HFD feeding compared to WT mice. In response to HFD, FHL2^{-/-} mice are protected against weight gain and hepatic steatosis, confirming our hypothesis that FHL2 has a substantial role in energy metabolism. We applied the whole-body FHL2-deficient mice, which may be considered a major limitation of current study. However, the overall beneficial

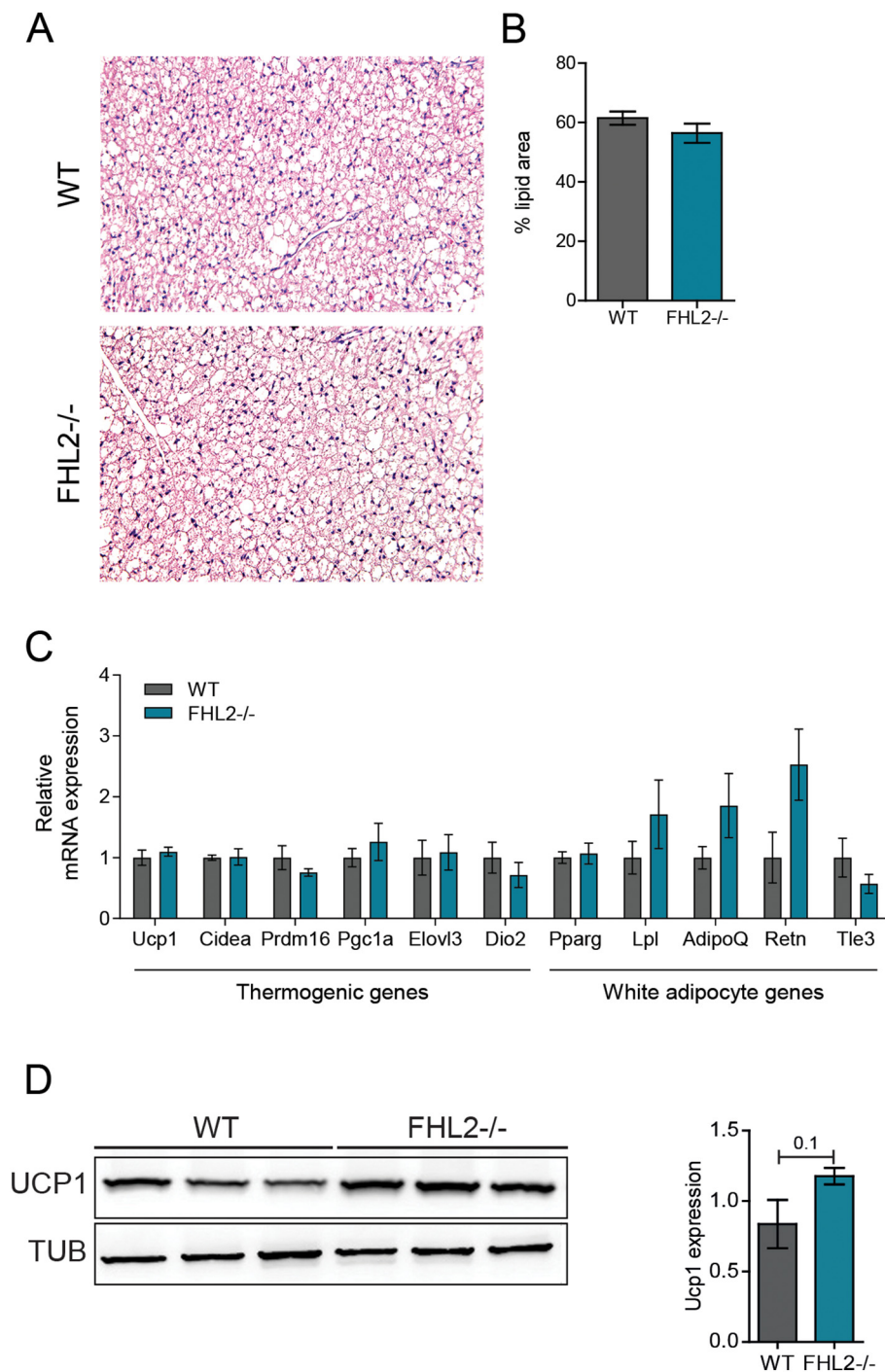


Fig. 5. Brown adipose tissue analysis.

(A) H&E staining of BAT from HFD mice.

(B) Quantification of total lipid area (n = 3).

(C) qPCR results for BAT thermogenic and white adipocyte genes (n = 4).

(D) UCP1 protein levels from WT and FHL2^{-/-} in BAT, Tubulin (TUB) used as loading control (n = 3).

Data are indicated as mean \pm SEM. p-values were calculated using two-tailed Student's *t*-test. *p < 0.05; **p < 0.01; ***p < 0.001. (For interpretation of the references to colour in this figure legend, the reader is referred to the web version of this article.)

phenotype we revealed is most likely determined by changes in multiple tissues, rather than by only one specific tissue or organ. This fits our present knowledge that FHL2 is expressed in various tissues and is a specific and often subtle modulator of several cellular signal transduction pathways. After only a few weeks of HFD the difference in weight gain between groups becomes already apparent with the body weight of FHL2^{-/-} mice remaining lower, whereas food intake and fecal

output are similar to wild-type mice. Together with the reduction in weight, hepatic steatosis is significantly reduced in the absence of FHL2. In line with the observation that silencing of FHL2 in an insulinoma cell line reduces insulin secretion [6], we observed that after HFD the fasting plasma insulin level is reduced in FHL2-deficient mice (Fig. 2C). However, there is no difference in glucose or insulin tolerance between WT and FHL2^{-/-} mice and also total insulin secretion

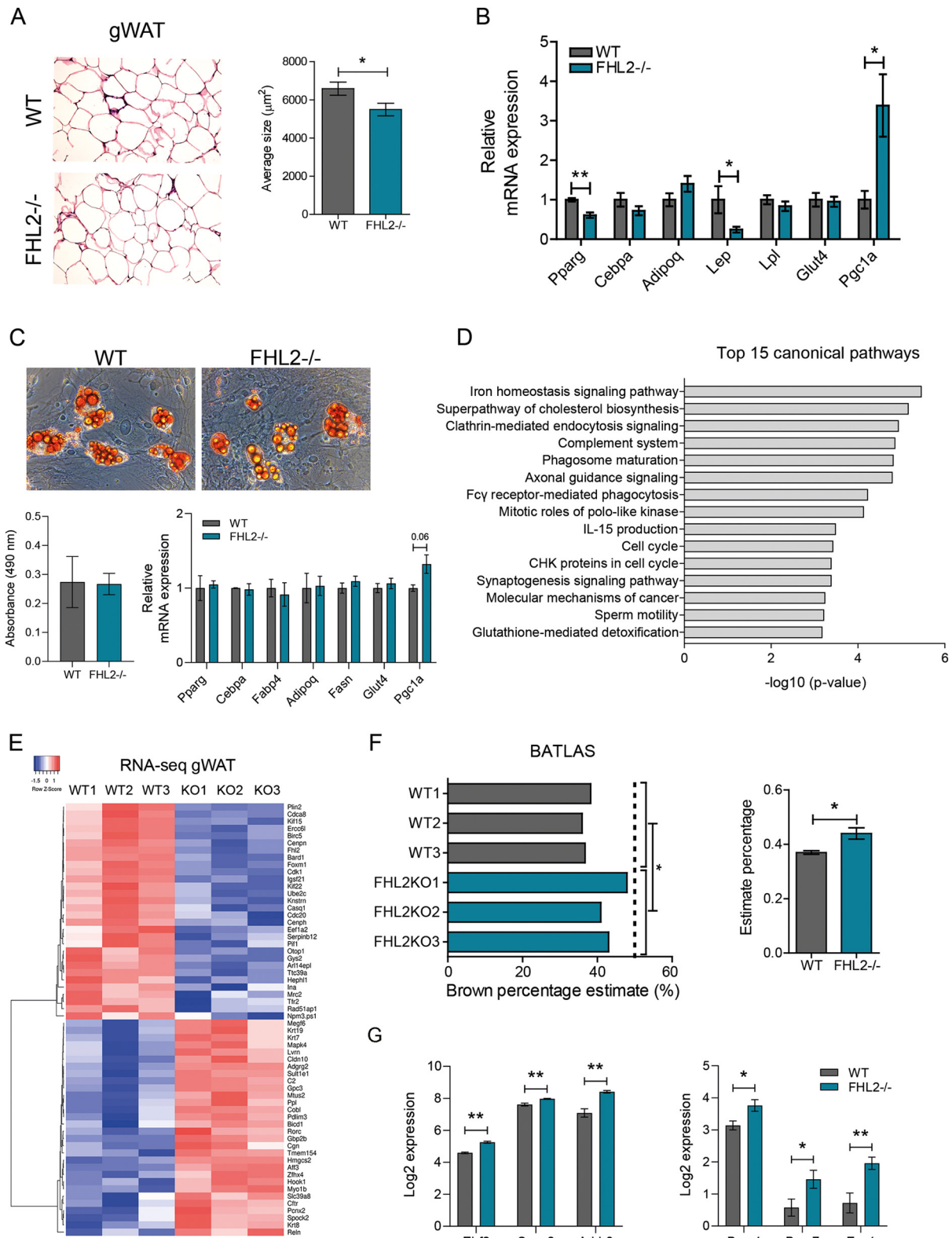


Fig. 6. WAT analysis from WT and FHL2-deficient mice revealing browning of WAT.

(A) H&E staining of gonadal white adipose tissue (gWAT) and quantification of the average size in µm².

(B) mRNA expression of typical WAT genes.

(C) Oil Red O staining and mRNA expression of adipogenic genes from WT and FHL2^{-/-} preadipocytes after 8 days of differentiation.

(D) Top 15 most significant canonical pathways from Ingenuity Pathway Analysis (IPA) of FHL2^{-/-} versus WT gWAT.

(E) Heatmap of the 30 top up- and down-regulated genes in RNA-seq data from FHL2^{-/-} versus WT gWAT.

(F) Individual browning percentage estimate based on BAT signature genes present in gWAT RNA-seq samples and average estimate percentage of browning.

(G) Ebf2, Syne2, Adrb3, Bmp4, Bmp7 and Eva1 gene expression in RNA-seq data from FHL2^{-/-} versus WT gWAT.

Data are indicated as mean ± SEM. p-values were calculated using two-tailed Student's t-test. *p < 0.05; **p < 0.01; ***p < 0.001. See also Fig. S4. (For interpretation of the references to colour in this figure legend, the reader is referred to the web version of this article.)

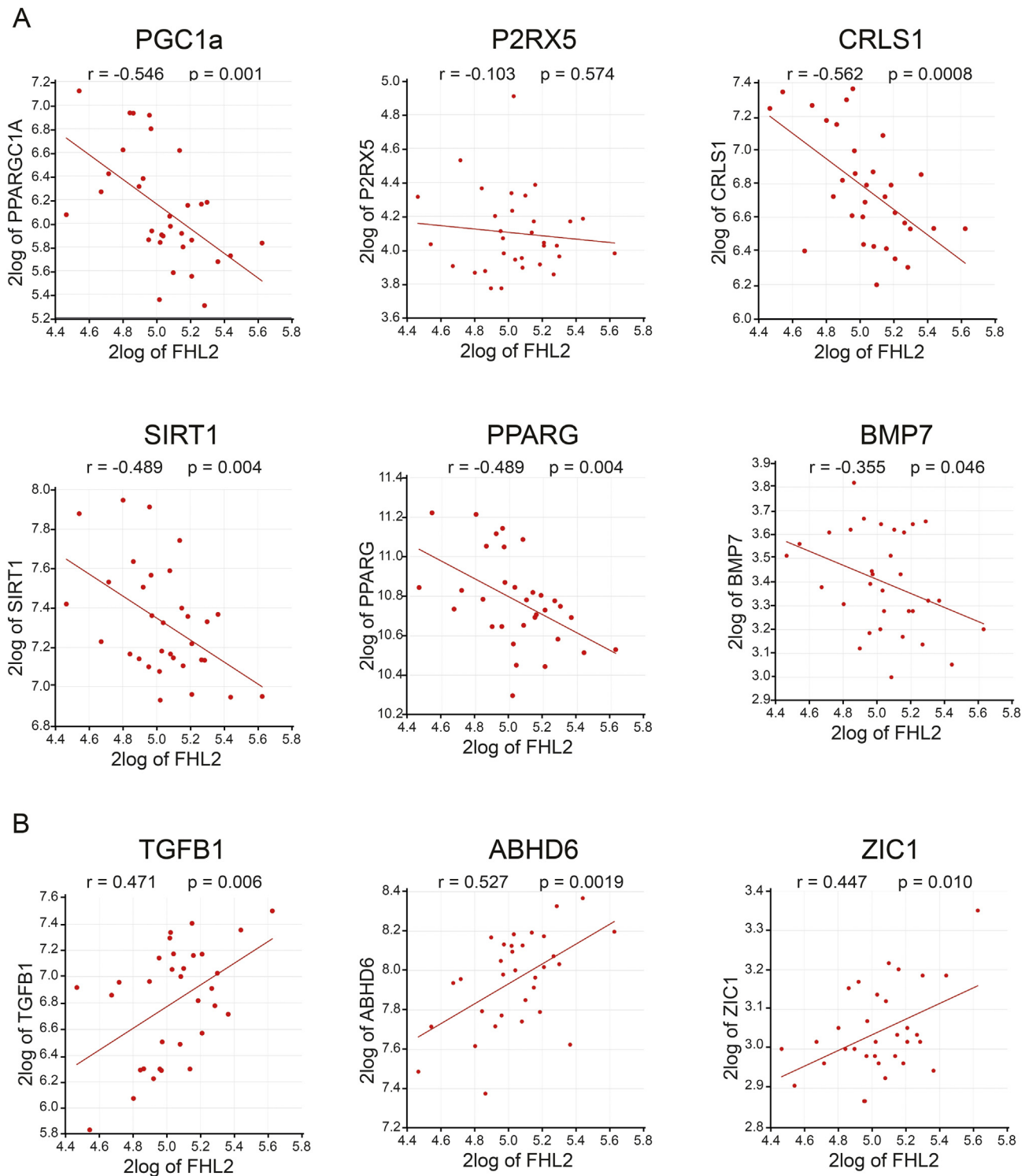


Fig. 7. Negative correlation of FHL2 expression with browning genes in human WAT from lean individuals and individuals with obesity.

(A) Negative correlation of expression of FHL2 (X-axis) and several genes involved in browning of WAT in subcutaneous WAT from lean individuals ($n = 16$) and individuals with obesity ($n = 16$) (from dataset GSE59034; female cohort). See also Fig. S5 and Table S4.

(B) Positive correlation of expression of FHL2 (X-axis) and genes involved in the inhibition of browning of WAT in subcutaneous WAT from lean individuals ($n = 16$) and individuals with obesity ($n = 16$) (from dataset GSE59034; female cohort). See also Fig. S5 and Table S4.

during the ipGTT is similar. Therefore, we conclude that glucose handling does not explain the difference in metabolic phenotype in response to HFD between WT and FHL2^{-/-} mice. Indirect calorimetry showed that heat production/energy expenditure is significantly higher in case of FHL2-deficiency under HFD conditions.

Given that FHL2 expression is highest in the heart [45], we decided to analyze this tissue in the setting of diet-induced obesity. The discovery of increased glucose uptake by the FHL2^{-/-} heart although not expected in this context, is in line with our knowledge that FHL2 deficiency promotes an exaggerated response in the heart when it is

challenged. This finding suggests that the diet and consequent weight gain can be considered a sufficient cardiac stressor to change the preferential substrate from fatty acid to glucose in the absence of FHL2, similar to a pathologic state. This was confirmed by transcriptomic analysis where several pathways involved in cardiac hypertrophy were listed. Analysis of possible upstream regulators based on differential gene expression from transcriptomic data, showed several activated regulators that have been described to regulate cell stress or have a role in heart failure. Among them we found MAPK1, which is an activated regulator found in FHL2^{-/-} heart, also a known as an interactor of FHL2. It was previously shown that FHL2 represses MAPK1 activity in cardiomyocytes and this was related to the cardiac hypertrophy response, but MAPK1 is also involved in glucose diffusion and development of insulin resistance in obesity [46,47].

Energy expenditure can be increased by the process of adaptive thermogenesis of BAT, but we found no structural differences, with a trend towards higher expression of the key thermogenic protein UCP1 in FHL2^{-/-} mice and a significant preference for the uptake from the circulation of fatty acids over glucose. It is noteworthy to mention that apart from the widely studied UCP1-dependent thermogenesis, there are other factors that contribute to the thermogenic machinery, such as calcium cycling, creatine signaling or UCP1-independent proton leak that could play a role in the study we present here [48].

When body composition is compared between the two mouse groups, the biggest difference relies in the amount of WAT, being consistently lower in various depots along the FHL2^{-/-} mouse body. Analyzing genome-wide expression of genes from gWAT the most remarkable difference is a strong upregulation of PGC1 α in the absence of FHL2. PGC1 α is a master regulator of mitochondrial biogenesis and energy expenditure, working as a coregulator of transcription in a wide variety of high energy-demanding metabolic tissues [49]. The role of PGC1 α is vastly described in BAT where its expression is induced upon cold stimuli. In the case of WAT, ectopic PGC1 α expression has been shown to induce browning of adipocytes providing them the ability of producing heat [50]. We pursued the white adipocyte browning hypothesis in FHL2^{-/-} gWAT resorting to RNA-seq and making use of BATLAS software, a useful tool to estimate the brown adipocyte content in a heterogeneous sample [32]. The results confirmed that the proportion of brown adipocyte signature gene expression was significantly higher in FHL2^{-/-} gWAT than in WT tissue, which is likely an important part of the energy expenditure increase observed. Importantly, in the absence of FHL2, expression of Adrb3 and Ebf2 genes in gWAT was remarkably higher than in WT. This may contribute to the browning phenotype of this tissue in mice since activation of both genes is known to drive brown fat induction in WAT [33,34].

We wish to highlight the fact that in FHL2^{-/-} mice increased expression of PGC1 α was found both in WAT and heart (the latter not shown) after HFD. Similar as for FHL2, the role of PGC1 α differs in a tissue-dependent context. Its function in BAT was already mentioned, but it is also known that fasting induces PGC1 α gene expression in the liver to increase the process of gluconeogenesis, or that in the skeletal muscle and cardiomyocytes it regulates metabolic homeostasis [52]. Therefore, the finding of an upregulation of PGC1 α gene across different tissues in our mouse model proposes the involvement of FHL2 in the co-regulation of PGC1 α gene transcription. Although regulation of PGC1 α gene expression varies depending on the tissue and energy requirements, it has been investigated that the PGC1 α promoter has specific binding sites for FoxO1, MEF2, CREB and ATF2, all of which enhance its transcription [49]. From this list of transcription regulators, FHL2 is known to interact with CREB and FoxO1 [8]. The interaction between FHL2 and CREB stimulates transcriptional activity of CREB target genes when co-expressed in mammalian cells [53], so in the hypothetical case that FHL2 was involved in PGC1 α transcription regulation it would not be through its interaction with CREB. On the other hand, FHL2 interacts with FoxO1 through deacetylase Sirt1 thereby inhibiting FoxO1 transcriptional activity [54], making it a plausible hypothesis for

PGC1 α increased expression in the absence of FHL2. Another possibility inferred from our data could be that the increase of Adrb3 expression in FHL2^{-/-} adipocytes causes a higher oxidative capacity upregulating genes involved in mitochondrial activity such as PGC1 α and inducing browning of WAT [55].

In the present study, we answered three main questions concerning FHL2. Firstly, does FHL2 have a role in energy metabolism and obesity development, secondly, what function could FHL2 be exerting in metabolically relevant tissues, and lastly are these observations relevant for human. The first question was successfully answered by confirming the advantageous phenotype of FHL2^{-/-} mice in comparison to wild type mice after HFD and next, we uncovered new roles for FHL2 in energy metabolism of heart and WAT. Finally, low FHL2 expression correlates with a lean phenotype in humans, adding FHL2 to the list of epigenetic factors involved in the development of this complex disease, in line with its role in obesity-related comorbidities.

CRediT authorship contribution statement

M.P.C.O. and C.J.dV. conceived the study and experiments. M.P.C.O., M.V., J.J.H., S.K. and R.O. performed the experiments. M.P.C.O. and A.J. performed and analyzed the high throughput sequencing (HTSeq) experiments. M.P.C.O. N.Z., P.C.N.R. and C.J.dV. wrote the manuscript. H.H., D.H.v.R., M.N., and E.C.E. provided expertise and feedback.

Declaration of competing interest

The authors declare no competing interests.

Acknowledgments

This research was supported by a grant from Rembrandt Institute of Cardiovascular Sciences and Research Institute Cardiovascular Sciences of Amsterdam UMC (C.J.dV.) and the Netherlands CardioVascular Research Initiative CVON-GENIUS-2 (P.C.N.R.). N.Z. is supported by a European Research Council Consolidator grant (617376). The graphical abstract was created with BioRender.com.

References

- [1] Locke AE, Kahali B, Berndt SI, Justice AE, Pers TH, Day FR, et al. Genetic studies of body mass index yield new insights for obesity biology. *Nature*. 2015. <https://doi.org/10.1038/nature14177>.
- [2] De Toro-Martín J, Guénard F, Tchermof A, Hould FS, Lebel S, Julien F, et al. Body mass index is associated with epigenetic age acceleration in the visceral adipose tissue of subjects with severe obesity. *Clin Epigenetics*. 2019. <https://doi.org/10.1186/s13148-019-0754-6>.
- [3] Jura M, Kozak LP. Obesity and related consequences to ageing. *Age (Omaha)*. 2016. <https://doi.org/10.1007/s11357-016-9884-3>.
- [4] Horvath S, Erhart W, Brosch M, Ammerpohl O, Von Schönfels W, Ahrens M, et al. Obesity accelerates epigenetic aging of human liver. *Proc Natl Acad Sci U S A*. 2014. <https://doi.org/10.1073/pnas.1412759111>.
- [5] Rönn T, Volkov P, Gillberg L, Kokosar M, Perflyev A, Jacobsen AL, et al. Impact of age, BMI and HbA1c levels on the genome-wide DNA methylation and mRNA expression patterns in human adipose tissue and identification of epigenetic biomarkers in blood. *Hum Mol Genet*. 2015. <https://doi.org/10.1093/hmg/ddv124>.
- [6] Bacos K, Gillberg L, Volkov P, Olsson AH, Hansen T, Pedersen O, et al. Blood-based biomarkers of age-associated epigenetic changes in human islets associate with insulin secretion and diabetes. *Nat Commun*. 2016. <https://doi.org/10.1038/ncomms11089>.
- [7] Bysani M, Perflyev A, De Mello VD, Rönn T, Nilsson E, Pihlajamäki J, et al. Epigenetic alterations in blood mirror age-associated DNA methylation and gene expression changes in human liver. *Epigenomics*. 2017. <https://doi.org/10.2217/epi-2016-0087>.
- [8] Tran MK, Kurakula K, Koenis DS, de Vries CJM. Protein-protein interactions of the LIM-only protein FHL2 and functional implication of the interactions relevant in cardiovascular disease. *Biochim Biophys Acta, Mol Cell Res*. 2016. <https://doi.org/10.1016/j.bbamc.2015.11.002>.
- [9] Kong Y, Shelton JM, Rothermel B, Li X, Richardson JA, Bassel-Duby R, et al. Cardiac-specific LIM protein FHL2 modifies the hypertrophic response to β -adrenergic stimulation. *Circulation*. 2001. <https://doi.org/10.1161/01.CIR.103.22.2731>.
- [10] Ramayo-Caldas Y, Ballester M, Fortes MRS, Esteve-Codina A, Castelló A, Noguera JL, et al. From SNP co-association to RNA co-expression: novel insights into gene networks for intramuscular fatty acid composition in porcine. *BMC Genomics*. 2014. <https://doi.org/10.1186/1471-2164-15-232>.

- [11] Kurakula K, Sommer D, Sokolovic M, Moerland PD, Scheij S, van Loenen PB, et al. LIM-only protein FHL2 is a positive regulator of liver X receptors in smooth muscle cells involved in lipid homeostasis. *Mol Cell Biol*. 2015. <https://doi.org/10.1128/mcb.00525-14>.
- [12] Petrus P, Meijert N, Corrales P, Lecoutre S, Li Q, Maldonado E, et al. Transforming growth factor- β 3 regulates adipocyte number in subcutaneous white adipose tissue. *Cell Rep*. 2018. <https://doi.org/10.1016/j.celrep.2018.09.069>.
- [13] Stááčaková A, Javorský M, Kuulasmaa T, Haffner SM, Kuusisto J, Laakso M. Changes in insulin sensitivity and insulin release in relation to glycemia and glucose tolerance in 6,414 Finnish men. *Diabetes*. 2009. <https://doi.org/10.2337/db08-1607>.
- [14] Civelek M, Wu Y, Pan C, Raulerson CK, Ko A, He A, et al. Genetic regulation of adipose gene expression and cardio-metabolic traits. *Am J Hum Genet*. 2017. <https://doi.org/10.1016/j.ajhg.2017.01.027>.
- [15] Govoni KE, Baylink DJ, Chen J, Mohan S. Disruption of four-and-a-half LIM 2 decreases bone mineral content and bone mineral density in femur and tibia bones of female mice. *Calcif Tissue Int*. 2006. <https://doi.org/10.1007/s00223-006-0074-7>.
- [16] Donato KA. Executive summary of the clinical guidelines on the identification, evaluation, and treatment of overweight and obesity in adults. *Arch Intern Med*. 1998. <https://doi.org/10.1001/archinte.158.17.1855>.
- [17] Wang S, Yehya N, Schadt EE, Wang H, Drake TA, Lusis AJ. Genetic and genomic analysis of a fat mass trait with complex inheritance reveals marked sex specificity. *PLoS Genet*. 2006. <https://doi.org/10.1371/journal.pgen.0020015>.
- [18] Wu CC, Huang HC, Juan HF, Chen ST. GeneNetwork: an interactive tool for reconstruction of genetic networks using microarray data. *Bioinformatics*. 2004. <https://doi.org/10.1093/bioinformatics/bth428>.
- [19] Kahn BB, Flier JS. Obesity and insulin resistance. *J Clin Invest*. 2000. <https://doi.org/10.1172/JCI10842>.
- [20] Chu PH, Yeh HI, Wu HH, Hong RC, Shiu TF, Yang CM. Deletion of the FHL2 gene attenuates the formation of atherosclerotic lesions after a cholesterol-enriched diet. *Life Sci*. 2010. <https://doi.org/10.1016/j.lfs.2010.01.007>.
- [21] Hojaye B, Rothermel BA, Gillette TG, Hill JA. FHL2 binds calcineurin and represses pathological cardiac growth. *Mol Cell Biol*. 2012. <https://doi.org/10.1128/mcb.05948-11>.
- [22] Kummitha CM, Kalhan SC, Saidel GM, Lai N. Relating tissue/organ energy expenditure to metabolic fluxes in mouse and human: experimental data integrated with mathematical modeling. *Physiol Rep*. 2014. <https://doi.org/10.14814/phy2.12159>.
- [23] Schulze PC, Drosatos K, Goldberg IJ. Lipid use and misuse by the heart. *Circ Res*. 2016. <https://doi.org/10.1161/CIRCRESAHA.116.306842>.
- [24] Neves FA, Cortez E, Bernardo AF, ABM Mattos, Vieira AK, Malafaia T de O, et al. Heart energy metabolism impairment in Western-diet induced obese mice. *J Nutr Biochem*. 2014. <https://doi.org/10.1016/j.jnutbio.2013.08.014>.
- [25] Freundt JK, Frommeyer G, Wötzel F, Hüge A, Hoffmeier A, Martens S, et al. The transcription factor ATF4 promotes expression of cell stress genes and cardiomyocyte death in a cellular model of atrial fibrillation. *Biomed Res Int*. 2018. <https://doi.org/10.1155/2018/3694362>.
- [26] Rashid HO, Yadav RK, Kim HR, Chae HJ. ER stress: autophagy induction, inhibition and selection. *Autophagy*. 2015. <https://doi.org/10.1080/15548627.2015.1091141>.
- [27] Suthahar N, Meijers WC, Silljé HHW, Ho JE, Liu FT, de Boer RA. Galectin-3 activation and inhibition in heart failure and cardiovascular disease: an update. *Theranostics*. 2018. <https://doi.org/10.7150/thno.22196>.
- [28] Zhang W, Elimban V, Nijjar MS, Gupta SK, Dhalla NS. Role of mitogen-activated protein kinase in cardiac hypertrophy and heart failure. *Exp Clin Cardiol Winter*. 2003;8(4):173-83.
- [29] Sackmann-Sala L, Berryman DE, Munn RD, Lubbers ER, Kopchick JJ. Heterogeneity among white adipose tissue depots in male C57BL/6J mice. *Obesity*. 2012. <https://doi.org/10.1038/oby.2011.235>.
- [30] Yook J-S, You M, Kim Y, Zhou M, Liu Z, Kim Y-C, et al. The thermogenic characteristics of adipocytes are dependent on the regulation of iron homeostasis. *J Biol Chem*. 2021. <https://doi.org/10.1016/j.jbc.2021.100452>.
- [31] Shen Q, Yasmeen R, Marbourg J, Xu L, Yu L, Fadda P, et al. Induction of innervation by encapsulated adipocytes with engineered vitamin A metabolism. *Transl Res*. 2018. <https://doi.org/10.1016/j.trsl.2017.10.005>.
- [32] Perdikari A, Leparic GG, Balaz M, Pires ND, Lidell ME, Sun W, et al. BATLAS: deconvoluting brown adipose tissue. *Cell Rep*. 2018. <https://doi.org/10.1016/j.celrep.2018.09.044>.
- [33] Jiang Y, Berry DC, Graff JM. Distinct cellular and molecular mechanisms for β 3 adrenergic receptor-induced beige adipocyte formation. *Elife*. 2017. <https://doi.org/10.7554/eLife.30329>.
- [34] Wang W, Kissig M, Rajakumari S, Huang L, Lim HW, Won KJ, et al. Eb2f is a selective marker of brown and beige adipogenic precursor cells. *Proc Natl Acad Sci U S A*. 2014. <https://doi.org/10.1073/pnas.1412685111>.
- [35] Shinoda K, Luijten IHN, Hasegawa Y, Hong H, Sonne SB, Kim M, et al. Genetic and functional characterization of clonally derived adult human brown adipocytes. *Nat Med*. 2015. <https://doi.org/10.1038/nm.3819>.
- [36] Elsen M, Raschke S, Tennagels N, Schwahn U, Jelenik T, Roden M, et al. BMP4 and BMP7 induce the white-to-brown transition of primary human adipose stem cells. *Am J Physiol Cell Physiol*. 2014. <https://doi.org/10.1152/ajpcell.00290.2013>.
- [37] Wu J, Boström P, Sparks LM, Ye L, Choi JH, Giang AH, et al. Beige adipocytes are a distinct type of thermogenic fat cell in mouse and human. *Cell*. 2012. <https://doi.org/10.1016/j.cell.2012.05.016>.
- [38] Okla M, Ha JH, Temel RE, Chung S. BMP7 drives human adipogenic stem cells into metabolically active beige adipocytes. *Lipids*. 2015. <https://doi.org/10.1007/s11745-014-3981-9>.
- [39] Sustarsic EG, Ma T, Lynes MD, Larsen M, Karavaeva I, Havelund JF, et al. Cardiolipin synthesis in brown and beige fat mitochondria is essential for systemic energy homeostasis. *Cell Metab*. 2018. <https://doi.org/10.1016/j.cmet.2018.05.003>.
- [40] Qiang L, Wang L, Kon N, Zhao W, Lee S, Zhang Y, et al. Brown remodeling of white adipose tissue by SirT1-dependent deacetylation of Ppar γ . *Cell*. 2012. <https://doi.org/10.1016/j.cell.2012.06.027>.
- [41] Kaisanlahti A, Glumoff T. Browning of white fat: agents and implications for beige adipose tissue to type 2 diabetes. *J Physiol Biochem*. 2019. <https://doi.org/10.1007/s13105-018-0658-5>.
- [42] Yadav H, Quijano C, Kamaraju AK, Gavrilo O, Malek R, Chen W, et al. Protection from obesity and diabetes by blockade of TGF- β /Smad3 signaling. *Cell Metab*. 2011. <https://doi.org/10.1016/j.cmet.2011.04.013>.
- [43] Zhao S, Mugabo Y, Ballentine G, Attane C, Iglesias J, Poursharifi P, et al. α / β -hydrolase domain 6 deletion induces adipose browning and prevents obesity and type 2 diabetes. *Cell Rep*. 2016. <https://doi.org/10.1016/j.celrep.2016.02.076>.
- [44] Zhang H, Huang Y, Lee HJ, Jin W. Zic1 negatively regulates brown adipogenesis in C3H10T1/2 cells. *Sci Bull*. 2015. <https://doi.org/10.1007/s11434-015-0797-9>.
- [45] Chu PH, Ruiz-Lozano P, Zhou Q, Cai C, Chen J. Expression patterns of FHL/SLIM family members suggest important functional roles in skeletal muscle and cardiovascular system. *Mech Dev*. 2000. [https://doi.org/10.1016/S0925-4773\(00\)00341-5](https://doi.org/10.1016/S0925-4773(00)00341-5).
- [46] Purcell NH, Darwis D, Bueno OF, Müller JM, Schüle R, Molkenin JD. Extracellular signal-regulated kinase 2 interacts with and is negatively regulated by the LIM-only protein FHL2 in cardiomyocytes. *Mol Cell Biol*. 2004. <https://doi.org/10.1128/mcb.24.3.1081-1095.2004>.
- [47] Bengal E, Aviram S, Hayek T. P38 mapk in glucose metabolism of skeletal muscle: beneficial or harmful? *Int J Mol Sci*. 2020. <https://doi.org/10.3390/ijms21186480>.
- [48] Roesler A, Kazak L. UCP1-independent thermogenesis. *Biochem J*. 2020. <https://doi.org/10.1042/BCJ20190463>.
- [49] Fernandez-Marcos PJ, Auwerx J. Regulation of PGC-1 α , a nodal regulator of mitochondrial biogenesis. *Am J Clin Nutr*. 2011. <https://doi.org/10.3945/ajcn.110.001917>.
- [50] Yuan D, Xiao D, Gao Q, Zeng L. PGC-1 α activation: a therapeutic target for type 2 diabetes? *Eat Weight Disord*. 2019. <https://doi.org/10.1007/s40519-018-0622-y>.
- [51] Cheng CF, Ku HC, Lin H. Pgc-1 α as a pivotal factor in lipid and metabolic regulation. *Int J Mol Sci*. 2018. <https://doi.org/10.3390/ijms19113447>.
- [52] Fimia GM, De Cesare D, Sassone-Corsi P. A family of LIM-only transcriptional coactivators: tissue-specific expression and selective activation of CREB and CREM. *Mol Cell Biol*. 2000. <https://doi.org/10.1128/mcb.20.22.8613-8622.2000>.
- [53] Yang Y, Hou H, Haller EM, Nicosia SV, Bai W. Suppression of FOXO1 activity by FHL2 through SIRT1-mediated deacetylation. *EMBO J*. 2005. <https://doi.org/10.1038/sj.emboj.7600570>.
- [54] Granneman JG, Li P, Zhu Z, Lu Y. Metabolic and cellular plasticity in white adipose tissue I: effects of β 3-adrenergic receptor activation. *Am J Physiol Endocrinol Metab*. 2005. <https://doi.org/10.1152/ajpendo.00009.2005>.